



Spatio-temporal
analyses of surface
ozone and
meteorology

J. Seo et al.

This discussion paper is/has been under review for the journal Atmospheric Chemistry and Physics (ACP). Please refer to the corresponding final paper in ACP if available.

Extensive spatio-temporal analyses of surface ozone and related meteorological variables in South Korea for 1999–2010

J. Seo^{1,3}, D. Youn², J. Y. Kim¹, and H. Lee⁴

¹Green City Technology Institute, Korea Institute of Science and Technology, Seoul, South Korea

²Department of Earth Sciences Education, Chungbuk National University, Cheongju, South Korea

³School of Earth and Environmental Science, Seoul National University, Seoul, South Korea

⁴Jet Propulsion Laboratory, California Institute of Technology, Pasadena, CA, USA

Received: 22 November 2013 – Accepted: 3 January 2014 – Published: 15 January 2014

Correspondence to: D. Youn (dyoun@chungbuk.ac.kr)

Published by Copernicus Publications on behalf of the European Geosciences Union.

Title Page

Abstract

Introduction

Conclusions

References

Tables

Figures



Back

Close

Full Screen / Esc

Printer-friendly Version

Interactive Discussion



Abstract

Spatio-temporal characteristics of surface ozone (O_3) variations over South Korea are investigated with consideration of meteorological factors and time-scales based on the Kolmogorov–Zurbenko filter (KZ-filter), using measurement data at 124 air quality monitoring sites and 72 weather stations for the 12 yr period of 1999–2010. In general, O_3 levels at coastal cities are high due to dynamic effects of the sea breeze while those at the inland and Seoul Metropolitan Area (SMA) cities are low due to the NO_x titration by local precursor emissions. We examine the meteorological influences on the O_3 using a combined analysis of the KZ-filter and linear regressions between O_3 and meteorological variables. We decomposed O_3 time-series at each site into short-term, seasonal, and long-term components by the KZ-filter and regressed them on meteorological variables. Impact of temperature on the O_3 levels is significantly high in the highly populated SMA and inland region while that is low in the coastal region. In particular, the probability of high- O_3 occurrence doubled with 4 °C of temperature increase in the SMA during high- O_3 months (May to October). It implies that those regions will experience frequent high- O_3 events in the future warming climate. In terms of short-term variation, distribution of high- O_3 probability classified by wind direction shows the effect of both local precursor emissions and long-range transport from China. In terms of long-term variation, the O_3 concentrations have increased by +0.26 ppbv yr⁻¹ on nationwide average, but their trends show large spatial variability. Additional statistical analysis of the singular value decomposition further reveals that the long-term temporal evolution of O_3 is similar to that of the nitrogen dioxide measurement although the spatial distributions of their trends are different. This study would be helpful as a reference for diagnostics and evaluation of regional- and local-scale O_3 and climate simulations and a guide to appropriate O_3 control policy in South Korea.

Spatio-temporal analyses of surface ozone and meteorology

J. Seo et al.

Title Page

Abstract

Introduction

Conclusions

References

Tables

Figures

⏪

⏩

◀

▶

Back

Close

Full Screen / Esc

Printer-friendly Version

Interactive Discussion



1 Introduction

Surface ozone (O_3) is a well-known secondary air pollutant, which affects air quality, human health, and vegetation. High O_3 concentration has detrimental effects on respiration, lung function, and airway reactivity in human health (Bernard et al., 2001; Bell et al., 2007). In terms of mortality, Levy et al. (2005) has previously assessed that 10 ppbv increase in 1 h maximum O_3 could increase daily mortality by 0.41 %. High O_3 concentrations could also reduce agricultural production. For example, Wang and Mauzerall (2004) reported that the East Asian countries of China, Japan, and South Korea lost 1–9 % of their yields of wheat, rice, and corn, and 23–27 % of their yields of soybeans due to O_3 in 1990. In addition, O_3 is one of greenhouse gases of which radiative forcing is estimated as the third largest contribution among the various constituents in the troposphere (IPCC, 2007). Therefore, the spatially inhomogeneous distribution of O_3 due to its short chemical lifetime of a week to a month could induce strong regional-scale climate responses (Mickley et al., 2004).

In the recent decades, tropospheric O_3 has increased in the Northern Hemisphere mainly due to increases in anthropogenic precursors, especially nitrogen oxides (NO_x) (Guicherit and Roemer, 2000; Vingarzan, 2004). In East Asia, there have been also growing concerns about elevated O_3 concentration owing to rapid economic growth and industrialization (e.g. Tang et al., 2009; Wang et al., 2009). The recent increases of O_3 in East Asia are also affected by transboundary transport of O_3 and its precursors. For example, previous modeling studies have shown that the transport of O_3 from China by continental outflow is one of the major contributions of O_3 in Japan and South Korea (Tanimoto et al., 2005; Nagashima et al., 2010). Intercontinental transport of O_3 and its precursors originated from East Asia affects O_3 concentration and related air quality in a remote area even on a global scale (Akimoto, 2003).

Recently, several studies have focused on the relationship between O_3 levels and temperature, and suggested potential influences of the global warming and climate change on the high levels of O_3 (Jacob and Winner, 2009; Rasmussen et al., 2012;

ACPD

14, 1191–1238, 2014

Spatio-temporal analyses of surface ozone and meteorology

J. Seo et al.

Title Page

Abstract

Introduction

Conclusions

References

Tables

Figures

⏪

⏩

◀

▶

Back

Close

Full Screen / Esc

Printer-friendly Version

Interactive Discussion

and references therein). Lin et al. (2001) calculated probability of daily 8 h maximum average O_3 exceeding 85 ppbv for a given range of daily maximum temperatures and reported that 3°C increase of the daily maximum temperature doubles risk of the O_3 exceedances in the Northeastern United States. In addition, Ordóñez et al. (2005) showed that high temperature extremes probably led to the high occurrence of severe O_3 episodes during the summer 2003 heat wave over Europe. These results imply the potentially large sensitivity of O_3 concentration and related air quality to the temperature increases (Jacob and Winner, 2009). In the model experiments by Lin et al. (2008), both averaged O_3 concentration and frequencies of high- O_3 episodes in the future were predicted to increase over the United States and East Asia. Based on climate-chemistry model experiments, Lei and Wang (2013) also have shown that O_3 production increases in warmer conditions in industrial regions over the United States.

In South Korea, one of the most highly populated countries in the world, both O_3 concentration and high- O_3 episodes have increased in recent decades despite efforts to regulate emissions of O_3 precursors (KMOE, 2012). Although the increase of O_3 levels in South Korea over the last three decades is mainly regarded as the results of rapid industrialization, economic expansion, and urbanization, there are other factors to be considered to explain the long-term increase in O_3 concentration. For example, since the Korean peninsula is located on the eastern boundary of East Asia, downward transport of O_3 by the continental outflow considerably affects the high O_3 levels in South Korea (Oh et al., 2010). In addition, recent warming trend related to the global climate change could also be an important factor to increase O_3 concentration in South Korea. The climate change is expected to increase both frequency and intensity of temperature extremes over the Korean peninsula (Boo et al., 2006). Therefore, comprehensive understanding of the various factors affecting O_3 concentration, such as local precursor emissions, transport of O_3 and its precursors from local and remote sources, and changes in meteorological fields related to the climate change is required to guide environmental policies.

Spatio-temporal analyses of surface ozone and meteorology

J. Seo et al.

[Title Page](#)[Abstract](#)[Introduction](#)[Conclusions](#)[References](#)[Tables](#)[Figures](#)[⏪](#)[⏩](#)[◀](#)[▶](#)[Back](#)[Close](#)[Full Screen / Esc](#)[Printer-friendly Version](#)[Interactive Discussion](#)

**Spatio-temporal
analyses of surface
ozone and
meteorology**

J. Seo et al.

Title Page

Abstract

Introduction

Conclusions

References

Tables

Figures

⏪

⏩

◀

▶

Back

Close

Full Screen / Esc

Printer-friendly Version

Interactive Discussion

The present study aims to examine the spatio-temporal characteristics of the measured O_3 variations in South Korea with consideration of three time-scales and various meteorological factors, using ground-measured data from 124 air quality monitoring sites and 72 weather stations for the 12 yr period of 1999–2010. We decomposed O_3 time-series at each measurement site into different time-scale of short-term, seasonal, and long-term components by application of the Kolmogorov–Zurbenko filter (KZ-filter) that has been used in previous studies (e.g. Gardner and Dorling, 2000; Ibarra-Berastegi et al., 2001; Thompson et al., 2001; Lu and Chang, 2005; Wise and Comrie, 2005; Tsakiri and Zurbenko, 2011; Shin et al., 2012). To investigate the meteorological impact on the O_3 levels, we applied the combined analysis of the KZ-filter and linear regression model with the meteorological variables. In the short-term time-scale, the possible effects of transport from the local and remote sources on the high- O_3 episodes were explored by using the wind data. In the long-term time-scale, the singular value decomposition (SVD) with nitrogen dioxide (NO_2) measurements was additionally applied to examine the effects of varying local emissions on the long-term O_3 trend.

The remainder of this paper is structured as follows. In the next section, we describe the observational data and analysis techniques used in this study. In Sect. 3, we investigated the spatio-temporal characteristics of the decomposed O_3 time-series and its relationship with meteorological variables over South Korea. Finally, the key findings are summarized in Sect. 4.

2 Data and methodologies

2.1 Data

Hourly data of O_3 and NO_2 mixing ratios in the unit of ppbv are provided for 290 air quality monitoring sites over South Korea by the National Institute of Environmental Research (NIER). The mixing ratios of O_3 and NO_2 at each monitoring site are measured

ρ times, which is denoted by $KZ_{m,\rho}$. The KZ-filter is basically low-pass filter of removing high frequency components from the original time-series. Following Eskridge et al. (1997), the KZ-filter removes the signal smaller than the period N , which is called as the effective filter width. N is defined as follows:

$$m \times \rho^{1/2} \leq N \quad (1)$$

The KZ-filter method has the same level of accuracy as the wavelet transform method although it is much easier way to decompose the original time-series (Eskridge et al., 1997). In addition, time-series with missing observations can be applicable to KZ-filter owing to the iterative moving average process.

The short-term components separated by the KZ-filter using daily O_3 time-series are not fully independent of the seasonal influence. We thus applied the KZ-filter to the daily time series of $\ln(O_3)$ as in Rao and Zurbenko (1994) and Eskridge et al. (1997). Applying $\ln(O_3)$ to the KZ-filter stabilizes variance of the short-term components because the KZ-filter can separates high-order nonlinear terms and effects into a short-term component (Rao and Zurbenko, 1994; Rao et al., 1997). Note that a temporal linear trend of log-transformed data is provided as $\% \text{ yr}^{-1}$ because the differential of the natural logarithm is equivalent to the percentage change.

The natural logarithm of the O_3 time-series at each site denoted as $[O_3](t)$ is thus decomposed by KZ-filter as follows:

$$[O_3](t) = [O_{3ST}](t) + [O_{3SEASON}](t) + [O_{3LT}](t) \quad (2)$$

$[O_{3ST}]$ is a short-term component attributable to day-to-day variation of synoptic-scale weather and short-term fluctuation in precursor emissions. $[O_{3SEASON}]$ represents a seasonal component related to the seasonal changes in solar radiation and vertical transport of O_3 from the stratosphere whose time scale is between several weeks to months. $[O_{3LT}]$ denotes a long-term component explained by changes in precursor emission, transport, climate, policy, and economy over the entire period (Rao et al., 1997; Milanchus et al., 1998; Gardner and Dorling, 2000; Thompson et al., 2001; Wise

Spatio-temporal analyses of surface ozone and meteorology

J. Seo et al.

[Title Page](#)[Abstract](#)[Introduction](#)[Conclusions](#)[References](#)[Tables](#)[Figures](#)[⏪](#)[⏩](#)[◀](#)[▶](#)[Back](#)[Close](#)[Full Screen / Esc](#)[Printer-friendly Version](#)[Interactive Discussion](#)

and Comrie, 2005). Tsakiri and Zurbenko (2011) showed that $[O_{3ST}]$ and $[O_{3LT}]$ are independent of each other. Also, statistical characteristics of $[O_{3ST}]$ are very close to those of white noise (Flaum et al., 1996) and therefore, $[O_{3ST}]$ is nearly detrended.

In this study, the KZ-filter with the window length of 29 days and 3 iterations ($KZ_{29,3}$) decomposed daily $\ln(O_{38h})$ time series at the 124 monitoring sites. $KZ_{29,3}$ removes $[O_{3ST}]$ of which the period is smaller than about 50 days, following Eq. (1). We defined the filtered time-series as a baseline ($[O_{3BL}]$) as in Eq. (3).

$$[O_3](t) = [O_{3BL}](t) + [O_{3ST}](t) \quad (3)$$

Equation (3) accounts for the multiplicative effects of short-term fluctuations on the $[O_{3BL}]$ due to the log-transformation (Thompson et al., 2001). In other words, exponential of $[O_{3ST}]$ is a ratio of the raw O_3 concentrations to the exponential of $[O_{3BL}]$, which is the baseline O_3 concentration in ppbv. Therefore, if $\exp[O_{3ST}]$ is larger than 1, the raw O_3 concentration will be larger than the baseline O_3 concentration.

$[O_{3BL}]$ is expressed as the sum of $[O_{3SEASON}]$ and $[O_{3LT}]$, as in Eq. (4) (Milanichus et al., 1998).

$$[O_{3BL}](t) = [O_{3SEASON}](t) + [O_{3LT}](t) \quad (4)$$

Since $[O_{3BL}]$ is closely associated with meteorological fields, we built a multiple regression model with available meteorological variables as in Eq. (5), following previous studies (e.g., Rao and Zurbenko, 1994; Rao et al., 1995; Ibarra-Berastegi et al., 2001). Short-term variability of meteorological variables was also filtered out by $KZ_{29,3}$.

$$[O_{3BL}](t) = a_0 + \sum_i a_i MET_{BL}(t)_i + \varepsilon(t) \quad (5)$$

$$MET_{BL}(t) = [T_{\max BL}(t), SI_{BL}(t), TD_{BL}(t), PS_{BL}(t), WS_{BL}(t), RH_{BL}(t)]$$

In the multiple linear regression model, $[O_{3BL}]$ is a response variable and the baselines of meteorological variables ($MET_{BL}(t)_i$) are predictors. Also, a_0 , a_i , and $\varepsilon(t)$ denote the

Spatio-temporal analyses of surface ozone and meteorology

J. Seo et al.

Title Page

Abstract

Introduction

Conclusions

References

Tables

Figures

⏪

⏩

◀

▶

Back

Close

Full Screen / Esc

Printer-friendly Version

Interactive Discussion



constant, regression coefficient of variable i , and residual of the multiple regression model, respectively.

The residual term $\varepsilon(t)$ contains not only the long-term variability of O_3 related to long-term changes in local precursor emissions but also seasonal variability of O_3 attributable to unconsidered meteorological factors in the multiple linear regression model. Thus, we applied the KZ-filter with the window length of 365 days and 3 iterations ($KZ_{365,3}$) to $\varepsilon(t)$ to extract the meteorologically adjusted $[O_{3LT}]$ of which the period is larger than about 1.7 yr as follow:

$$\varepsilon(t) = KZ_{365,3}[\varepsilon(t)] + \delta(t) = [O_{3LT}](t) + \delta(t) \quad (6)$$

In Eq. (6), $\delta(t)$ denotes the seasonal variability of O_3 related to the meteorological variables unconsidered in the multiple linear regression model and/or noise.

Finally, $[O_{3SEASON}]$ is obtained by the sum of total meteorological effects regressed on $[O_{3BL}]$ ($a_0 + \sum_i a_i MET_{BL}(t)_i$) and meteorological effects of which the period is larger than 50 days but smaller than 1.7 yr ($\delta(t)$) as in Eq. (7).

$$[O_{3SEASON}](t) = a_0 + \sum_i a_i MET_{BL}(t)_i + \delta(t) \quad (7)$$

Figure 2 shows a schematic representation of Eq. (2) using daily O_{38h} time-series at the City Hall of Seoul for the period of 1999–2010. $[O_{3SEASON}]$ in Fig. 2c clearly shows typical seasonal cycle of O_3 in South Korea with high concentrations in spring, slight decrease in July and August, and increase in autumn (Ghim and Chang, 2000). The spring maximum of O_3 concentration in the Northern Hemisphere is generally attributed to episodic stratospheric intrusion (Levy et al., 1985; Logan, 1985), photochemical reactions of accumulated NO_x and hydrocarbons during the winter (Dibb et al., 2003), accumulation of O_3 due to the longer photochemical lifetime (~ 200 days) during the winter (Liu et al., 1987), and transport of O_3 and its precursors by the continental outflow (Carmichael et al., 1998; Jacob et al., 1999; Jaffe et al., 2003). On the other hand, frequent precipitation during the East Asian summer monsoon influences the decrease

of O₃ concentrations in July and August (Ghim and Chang, 2000). [O_{3LT}] in Fig. 2d shows that the O₃ concentrations at the monitoring site have increased in the past decade, irrespective of any change in meteorological conditions.

2.3 Spatial interpolation by AIDW method

The inverse-distance weighting (IDW) is a deterministic spatial interpolation technique for spatial mapping of variables distributed at irregular points. In this study, we adopted the enhanced version of the IDW, the adaptive inverse-distance weighting (AIDW) technique (Lu and Wong, 2008). While the traditional IDW uses a fixed distance-decay parameter without considering the distribution of data within it, the AIDW uses adjusted distance-decay parameters according to density of local sampling points. Therefore, the AIDW provides flexibility to accommodate variability in the distance-decay relationship over the domain and thus better spatial mapping of variables distributed at irregular observational points (Lu and Wong, 2008).

In the mapping of O₃ with spatial interpolation, there are ubiquitous problems such as spatial-scale violations, improper evaluations, inaccuracy, and inappropriate use of O₃ maps in certain analyses (Diem, 2003). The spatial mapping in the present study also has problems with the spatial resolution of the observation, which is not high enough to consider small-scale chemical processes and geographical complexity of the Korean peninsula (see Fig. 1). Most of the air quality monitoring sites are concentrated on the cities, and typical inter-city distances are 30–100 km in South Korea while spatial representativeness of O₃ concentration is possibly as small as around 3–4 km (Tilmes and Zimmermann, 1998) or 5 km (Diem, 2003). Despite such limits, the spatial mapping in this study is still useful because we aim not to derive an exact value at a specific point where the observation does not exist, but to provide the better quantitative understanding of O₃ and related factors in South Korea, especially focused on the metropolitan and urban areas.

Spatio-temporal analyses of surface ozone and meteorology

J. Seo et al.

Title Page

Abstract

Introduction

Conclusions

References

Tables

Figures

⏪

⏩

◀

▶

Back

Close

Full Screen / Esc

Printer-friendly Version

Interactive Discussion

3 Results

3.1 Spatial characteristics of O₃ and its trend in South Korea

Climatological daily average O₃ (O_{3avg}) and its temporal linear trends are represented in Fig. 3 and Table 1 using data from 124 monitoring sites distributed nationwide in 46 cities for the past 12 yr period. The spatial map of climatological daily average NO₂ (NO_{2avg}) is also shown in Fig. 3. In Table 1, the cities are categorized into three geographical groups: 16 coastal cities, 14 inland cities, and 16 cities in the Seoul Metropolitan Area (SMA). We separated the SMA cities from the other two groups since the SMA is the largest source region of anthropogenic O₃ precursors in South Korea. The SMA occupies only 11.8 % (11 745 km²) of the national area, but has 49 % (25.4 million) of the total population and 45 % (8.1 million) of total vehicles in South Korea. It is estimated that approximately 27 % (291 kt) of total NO_x emissions and 34 % (297 kt) of the volatile organic compounds (VOCs) emissions in South Korea are from the SMA in 2010 (KMOE, 2013). Therefore, the climatological NO_{2avg} concentration in the SMA is much higher than that in other region (Fig. 3b).

In general, O₃ concentrations are high at the coastal cities, low at the inland cities, and lowest at the SMA cities in South Korea. Along with Table 1, Fig. 3a shows that the 12 yr average of O_{3avg} is high at the southern coastal cities such as Jinhae (31.3 ppbv), Mokpo (30.3 ppbv), and Yeosu (28.1 ppbv), with the highest value at Jeju (32.6 ppbv), and low at the inland metropolitan cities such as Daegu (19.8 ppbv), Gwangju (20.5 ppbv), and Daejeon (20.7 ppbv), with lowest values at the SMA cities including Seoul (17.1 ppbv), Incheon (19.0 ppbv) and Anyang (16.8 ppbv).

Compared to the regional background concentration of 35–45 ppbv at five background measurement sites around South Korea (KMOE, 2012), the averaged O₃ concentrations in the SMA and inland metropolitans are much lower while those at the coastal cities are close to the regional background levels. In comparison with Fig. 3b, Fig. 3a shows that relatively lower O_{3avg} regions are well consistent with relatively

Title Page

Abstract

Introduction

Conclusions

References

Tables

Figures



Back

Close

Full Screen / Esc

Printer-friendly Version

Interactive Discussion

higher $\text{NO}_{2\text{avg}}$ region. Substantial emissions of anthropogenic NO in the SMA and other inland metropolitans lead NO_x titration effects even in the absence of photochemical reactions during the night, and thus the averaged O_3 concentrations are depressed by 10–20 ppbv lower than the regional background concentration (Ghim and Chang, 2000). A recent modeling study by Jin et al. (2012) has suggested that the maximum O_3 concentrations in the SMA, especially in Seoul and Incheon, are VOCs-limited. In the coastal region, on the other hand, low emissions of NO with dilution by the strong winds weaken the titration effect and result in the high O_3 concentrations. The dynamic effect of land-sea breeze is another possible factor of the high O_3 levels at the coastal cities. Oh et al. (2006) showed that a near-stagnant wind condition at the development of sea breeze temporarily contains O_3 precursors carried by the offshore land breeze during the night, and following photochemical reactions at mid-day produces O_3 . The relationship between O_3 and wind speed and direction will be shown in Sects. 3.2 and 3.5 respectively.

In terms of temporal trends, the surface O_3 concentrations in South Korea have generally increased for the past 12 yr as shown in Fig. 3c and Table 1. The averaged temporal linear trend of $\text{O}_{3\text{avg}}$ at 46 cities nationwide is $+1.15\% \text{ yr}^{-1}$ ($+0.26 \text{ ppbv yr}^{-1}$), which is comparable with observed increasing trends of approximately $+0.5\text{--}2\% \text{ yr}^{-1}$ in various regions in the Northern Hemisphere (Vingarzan, 2004). Compared with previous studies in East Asia, the overall increasing trend of O_3 in South Korea is smaller than recent increasing trends over China of $+1.1 \text{ ppbv yr}^{-1}$ in Beijing for 2001–2006 (Tang et al., 2009) and $+0.58 \text{ ppbv yr}^{-1}$ in Hong Kong for 1994–2007 (Wang et al., 2009) but slightly larger than increasing trend over Japanese populated areas of $+0.18 \text{ ppbv yr}^{-1}$ for 1996–2005 (Chatani and Sudo, 2011).

Several factors that could influence the overall increase of O_3 over East Asia were suggested by the following previous studies. Tanimoto et al. (2009) suggested that the O_3 increase results from recently increased anthropogenic precursor emissions in East Asia. However, model sensitivity simulations in Chatani and Sudo (2011) indicate that the changes in East Asian emissions can explain only 30 % of the O_3 trend. They have

**Spatio-temporal
analyses of surface
ozone and
meteorology**

J. Seo et al.

Title Page

Abstract

Introduction

Conclusions

References

Tables

Figures

⏪

⏩

◀

▶

Back

Close

Full Screen / Esc

Printer-friendly Version

Interactive Discussion

influence of insolation on O_3 levels by photochemical production (Dawson et al., 2007; and references therein). The apparent R^2 differences among three regions indicate that temporal variations of O_3 at the SMA and inland cities are much more sensitive to SI and T_{\max} than those at the coastal cities. The low dependence of O_3 on T_{\max} and SI at the coastal cities means that the photochemical reactions of precursors are less important for determining O_3 levels there compared to the SMA and inland cities.

The meteorological effects on O_3 at the inland, coastal, and SMA cities are also examined by daily minimum O_3 ($O_{3\min}$). In the polluted urban area, the O_3 concentration reaches near-zero minima during the night since O_3 is reduced by NO_x titration and dry deposition in the absence of photochemical reactions. However, if O_3 is persistently transported from the high- O_3 background, the concentrations will keep higher levels even at the nighttime (Ghim and Chang, 2000). Therefore, the high $O_{3\min}$ near the coast (see Fig. 6a and Table 3) implies the large influences of the background O_3 transport at the coastal cities. Previous analyses of frequency distributions of O_3 concentrations have also shown that the O_3 levels at the coastal cities such as Gangneung, Jeju, Mokpo, Seosan, and Yeosu are affected by the background O_3 transport different from Seoul where the effect of local precursor emission is dominant (Ghim and Chang, 2000; Ghim, 2000).

Compared to the spatial distribution of R^2 between O_3 and T_{\max} or SI in Fig. 5a and b, $O_{3\min}$ distribution in Fig. 6a shows high $O_{3\min}$ at the coastal cities where the R^2 is low and low $O_{3\min}$ at the inland cities where the R^2 is high. These opposite patterns suggest that the meteorological effects on the O_3 production and transport effects of background O_3 are negatively correlated for the South Korean cities. The clear negative correlations are also shown in scatter plots (Fig. 6b and c). In both two scatter plots, the three geographical groups of cities (blue for the coastal cities, green for the inland cities and red for SMA) are well separated. Several industrial or metropolitan cities in the coastal region such as Changwon (CW), Busan (BS), and Ulsan (US) have relatively low $O_{3\min}$ compared to the rest of coastal cities. Larger NO_x emissions in these southeastern coastal cities (Fig. 3b) induce lower $O_{3\min}$ levels via

Spatio-temporal analyses of surface ozone and meteorology

J. Seo et al.

Title Page

Abstract

Introduction

Conclusions

References

Tables

Figures

⏪

⏩

◀

▶

Back

Close

Full Screen / Esc

Printer-friendly Version

Interactive Discussion

Spatio-temporal analyses of surface ozone and meteorology

J. Seo et al.

Title Page

Abstract

Introduction

Conclusions

References

Tables

Figures

⏪

⏩

◀

▶

Back

Close

Full Screen / Esc

Printer-friendly Version

Interactive Discussion

almost doubled by about 4 °C increase in T_{\max} and reach 27 % at 30 °C. In the coastal region, on the other hand, the probability of O_3 exceedance increases up to 12–13 % with T_{\max} change from 10 °C to 20 °C and does not increase significantly for T_{\max} above 20 °C. This is consistent with the spatial feature of the meteorological effects on O_3 levels, which are high at the inland and SMA cities and low at the coastal cities as described in the previous section. Therefore, the probability of high O_3 occurrence will be more sensitive to the future climate change at the inland and SMA cities than at the coastal cities. In the previous modeling study by Boo et al. (2006), T_{\max} over the Korean peninsula is expected to rise by about 4–5 °C to the end of 21st century owing to the global warming. This indicates considerable future increases in exceedances of the O_3 air quality standard over South Korea except coastal regions.

3.4 Relative contributions of O_3 variations in different time-scales

Surface O_3 variation can be decomposed into short-term component ($[O_{3ST}]$), seasonal component ($[O_{3SEASON}]$), and long-term component ($[O_{3LT}]$) by using the KZ-filter as described in Sect. 2.2. We evaluated relative contributions of each component to total variance of original time-series. Overall, the relative contributions of $[O_{3LT}]$ in Fig. 9c are much smaller than those of $[O_{3ST}]$ in Fig. 9a and $[O_{3SEASON}]$ in Fig. 9b at all cities (Table 4). Therefore, sum of $[O_{3ST}]$ and $[O_{3SEASON}]$ account for the most of O_3 variations.

In Fig. 9a and b, the relative contributions of $[O_{3ST}]$ and $[O_{3SEASON}]$ show a strong negative relationship spatially. The relative contributions of $[O_{3ST}]$ are generally large at the coastal cities (53.1 %) and small at the inland cities (45.9 %), whereas the relative contributions of $[O_{3SEASON}]$ are small at the coastal cities (32.8 %) and large at the inland cities (41.9 %). Since $[O_{3ST}]$ is related to synoptic-scale weather fluctuation by transport of O_3 (Rao et al., 1995, 1997), the large relative contributions of $[O_{3ST}]$ at the coastal cities indicate the stronger effects of the synoptic-scale transport of background O_3 there. On the other hand, $[O_{3SEASON}]$ is driven mainly by the annual cycle of meteorological factors such as insolation or temperature. Therefore, the large relative

contributions of $[O_{3SEASON}]$ at the inland cities are consistent with the higher impacts of temperature and insolation on the O_3 therein (Figs. 5 and 9b). $[O_{3LT}]$ explain less than 10 % of the total variances, but its relative contribution is considerable in the south-western part of the Korean peninsula as displayed in Fig. 9c. This is related to relatively large long-term variability or trend in the region and is further discussed in Sect. 3.6.

3.5 Short-term variation of O_3 related to wind direction

The short-term components of O_3 ($[O_{3ST}]$) account for a large fraction of total O_3 variation over South Korea. In Table 4, relative contributions of $[O_{3ST}]$ range from 32.7 % to 62.5 % and have a nationwide average of 49.8 %. Therefore, it is no wonder that high- O_3 episodes are mostly determined by day-to-day fluctuation of $[O_{3ST}]$. One considerable factor influencing the short-term variation of O_3 is wind. Shin et al. (2012) displayed $[O_{3ST}]$ on the wind speed-direction domain and showed that the effects of episodic long-range transport and local precursor emission on the ambient O_3 concentrations could be qualitatively separated from $[O_{3ST}]$.

We here further investigate the transport effect on the short-term variations of O_3 and the frequency of high- O_3 episodes using $\exp[O_{3ST}]$ and wind directions (WDs). As described in Sect. 2.2, $\exp[O_{3ST}]$ is a ratio of the raw O_{38h} concentration to its baseline concentration in ppbv ($\exp[O_{3BL}]$). Thus, the O_{38h} concentration is higher than the baseline O_{38h} concentration when $\exp[O_{3ST}] > 1$. We classified every single value of $\exp[O_{3ST}]$ by 8 cardinal WDs during the high- O_3 season (May–October) at all available monitoring sites within each city. The probabilities of $\exp[O_{3ST}] > 1$ by each WD were compared with the probabilities exceeding the South Korean air quality standard of 60 ppbv for O_{38h} .

Figure 10 shows $\exp[O_{3ST}]$ in the SMA cities (Seoul, Incheon, Suwon, and Ganghwa) with probabilities of $\exp[O_{3ST}] > 1$ and $O_{38h} > 60$ ppbv for each WD. In Seoul, high- O_3 episodes are occurred most in northwesterly although westerly and northeasterly winds predominate during the high- O_3 season (Fig. 10a and b). The high probability of high- O_3 in northwesterly in Seoul is similar to those in other neighboring cities in

Title Page

Abstract

Introduction

Conclusions

References

Tables

Figures

◀

▶

◀

▶

Back

Close

Full Screen / Esc

Printer-friendly Version

Interactive Discussion



SMA, where the predominant probability also appears in northwesterly wind in Incheon located in the west of Seoul (Fig. 10c and d), westerly wind in Suwon in the south of Seoul (Fig. 10e and f), and Ganghwa in the northwest of Seoul (Fig. 10g and h).

Sea–mountain breeze can explain the prevalence of high-O₃ episodes under west or northwesterly winds in the SMA. In the western coast of the SMA, there are many thermoelectric power plants (see triangles in Figs. 11 and 12) and industrial complexes where directly emit a large amount of O₃ precursors. Heavy inland and maritime transportation in those regions are also important source of NO_x and hydrocarbon emissions. Since the SMA is surrounded by the Yellow Sea in the west and mountainous region in the east (see Fig. 1), the westerly sea breeze are well developed under O₃-conductive meteorological conditions such as high temperature and strong insolation with low wind speed (Ghim and Chang, 2000; Ghim et al., 2001). In addition, locally emitted precursors and transported background O₃ from the west are trapped in the SMA due to the westerly sea breeze and the mountainous terrain in the east of the SMA. Therefore, the O₃ concentrations in the SMA increase in such O₃-conductive meteorological conditions with near-westerly winds.

Another factor to increase the high-O₃ probabilities in the near-westerly winds is long-range transport of O₃ and its precursors from China. For example, Ghim et al. (2001) reported some high-O₃ cases in the SMA, which result from the transport of O₃-rich air with strong westerly wind at dawn under overcast conditions. Oh et al. (2010) also showed that the elevated layer of high O₃ concentration over the SMA is associated with the long-range transport of O₃ from eastern China. As the mixing layer thickens over the SMA, the O₃ concentration can increase by up to 25 % via vertical down-mixing process (Oh et al., 2010). Recently, Kim et al. (2012) showed that westerly winds also transport O₃ precursors such as NO₂ and carbon monoxide (CO) from China to South Korea.

Interestingly, the high-O₃ probability in Ganghwa (Fig. 10g and h) shows bimodal distribution with another peak in easterly wind. Considering that Ganghwa is a rural

Spatio-temporal analyses of surface ozone and meteorology

J. Seo et al.

Title Page

Abstract

Introduction

Conclusions

References

Tables

Figures

⏪

⏩

◀

▶

Back

Close

Full Screen / Esc

Printer-friendly Version

Interactive Discussion

county on the northwestern coast of the SMA, the double peak of high-O₃ probability in easterly and westerly winds shows the effects of both local and long-range transport.

We extended the above exp[O_{3ST}] and WDs analysis to 25 cities over South Korea. The nationwide view of the high-O₃ probabilities is represented by the probabilities of exp[O_{3ST}] > 1 and O_{38h} > 60 ppbv by each wind direction during the high-O₃ season (May–October). Figures 11 and 12 show spatial maps of the probabilities of exp[O_{3ST}] > 1 and O_{38h} > 60 ppbv, respectively. As indicators of major precursor emission point source, we marked 26 of major thermoelectric power plants with triangles on the map. In general, the most of the thermoelectric power plants are located in the western coast of the SMA and southeastern coastal region of the Korean peninsula. Thermoelectric power plants are important sources of NO_x in South Korea, accounting for 13% (140 kt) of total NO_x emission nationwide (KMOE, 2013). Considering that industrial complexes over South Korea are mostly concentrated near the power plants, the area with triangles in Figs. 11 and 12 represents major sources of O₃ precursors.

In Figs. 11 and 12, the both probabilities of exp[O_{3ST}] > 1 and O_{38h} > 60 ppbv are generally high on a national scale in the near-westerly wind conditions (Figs. 11f–h and 12f–h). The prevailing westerly wind of the synoptic-scale flow transports O₃ and its precursors from China to South Korea and thus increases the probability of high-O₃ episodes as well as high O₃ concentrations. However, on a local scale, the high probability regions of high-O₃ correspond to downwind of the thermoelectric power plants. For example, the high probabilities of high-O₃ in the southeastern part of South Korea, downwind of power plants along the southeastern coast, also appear even in the easterly or southerly wind (Figs. 11c–e and 12c–e). Therefore, the spatial features of the high-O₃ probabilities in each wind direction could be associated with both local effect of precursor emission and long-range transport from the continent.

3.6 Long-term variation of O₃ and local precursor emissions

Temporal linear trend of baseline ([O_{3BL}]) is almost same with that of the original time-series since short-term component ([O_{3ST}]) is nearly detrended. Therefore, the O₃

Spatio-temporal analyses of surface ozone and meteorology

J. Seo et al.

Title Page

Abstract

Introduction

Conclusions

References

Tables

Figures



Back

Close

Full Screen / Esc

Printer-friendly Version

Interactive Discussion



Spatio-temporal analyses of surface ozone and meteorology

J. Seo et al.

Title Page

Abstract

Introduction

Conclusions

References

Tables

Figures

⏪

⏩

◀

▶

Back

Close

Full Screen / Esc

Printer-friendly Version

Interactive Discussion

trend can be represented as a sum of the seasonal component ($[O_{3SEASON}]$) and long-term component ($[O_{3LT}]$) trends. The spatial trend distributions of $[O_{3BL}]$ and its two separated components of seasonal and long-term components are shown in Fig. 13. It is noted that the period used in Fig. 13 is shorter than the total period of original data because of truncation effect in the KZ-filter process. The long-term component obtained by the KZ-filter of $KZ_{365,3}$ loses 546 days at the beginning and end of original time-series.

The increasing trends of O_3 are generally high in the SMA and southwestern part and low in the southeastern coastal region of Korean peninsula (Fig. 13a). This spatial inhomogeneity of the O_3 trends over South Korea is mainly contributed by the long-term component trends (Fig. 13c) rather than the seasonal component trend (Fig. 13b). Therefore, the large spatial variability in local precursor emissions induced the spatial inhomogeneity of O_3 trends in South Korea. On the other hand, relatively homogeneous distribution of the seasonal component trends implies that meteorological influences on the long-term changes in O_3 have little regional dependence nationwide.

Since the spatially inhomogeneous O_3 trends are related to the local precursor emissions, we also tried to investigate their relationship with NO_2 measurement data. To detect temporally synchronous and spatially coupled patterns between the long-term variations of O_3 and NO_2 , we applied the SVD to $[O_{3LT}]$ and the long-term component of NO_2 ($[NO_{2LT}]$). $[NO_{2LT}]$ was simply obtained by applying the KZ-filter of $KZ_{365,3}$ to the log-transformed NO_2 time-series. The SVD is usually applied to two combined space-time data fields, based on the computation of a temporal cross-covariance matrix between two data fields. The SVD identifies coupled spatial patterns and their temporal variations, with each pair of spatial patterns explaining a fraction of the square covariance between the two space-time data sets. The square covariance fraction (SCF) is largest in the first pair (mode) of the patterns, and each succeeding mode has a maximum SCF that is unexplained by the previous modes.

The first three leading SVD modes (singular vectors) of the coupled O_3 and NO_2 long-term components account for the SCF with 94.6% of the total, of which the first,

(+1.15 % yr⁻¹). The recent increase of the O₃ levels, which is common in the Northern Hemisphere and East Asia, may result from the recent increase of anthropogenic precursor emissions in East Asia and the long-term variations in meteorological effects.

We applied a linear regression model to investigate the relationships between O₃ and meteorological variables such as temperature, insolation, dew-point temperature, sea-level pressure, wind speed, and relative humidity. Spatial distribution of the R² values shows high meteorological influences in the SMA and inland regions and low meteorological influences in the coastal region. The high meteorological influences in the SMA and inland regions are related to effective photochemical activity, which results from large local precursor emissions and stagnant condition with low wind speeds. On the other hand, the low meteorological influences in the coastal region are related to large transport effects of the background O₃ and ventilation and dry deposition with high wind speeds.

In the SMA and inland region, the high-O₃ probability (O_{38h} > 60 ppbv) increases with the daily maximum temperature rise. Specifically in the SMA, the most populated area in South Korea, the probability of the O₃ exceedances is almost doubled for about 4 °C increase in daily maximum temperature and reached 27 % at 30 °C. It is noted that the variations in O₃ exceedance probabilities according to the maximum temperature show an approximate logarithmic increase in the SMA and inland regions. It thus implies that these regions will experience more frequent high-O₃ events in the future climate conditions with the increasing global temperature.

The O₃ time-series observed at each monitoring site can be decomposed into the short-term, seasonal, and long-term components by the KZ-filter. Relative contributions of each separated component show that the short-term and seasonal variations account for most of the O₃ variability. Relative contributions of the short-term component are large at the coastal cities due to influence of the background O₃ transport. In contrast, those of the seasonal component are large at the inland cities due to the high meteorological influences on the O₃ variations.

Spatio-temporal analyses of surface ozone and meteorology

J. Seo et al.

Title Page

Abstract

Introduction

Conclusions

References

Tables

Figures

⏪

⏩

◀

▶

Back

Close

Full Screen / Esc

Printer-friendly Version

Interactive Discussion



**Spatio-temporal
analyses of surface
ozone and
meteorology**

J. Seo et al.

Title Page

Abstract

Introduction

Conclusions

References

Tables

Figures



Back

Close

Full Screen / Esc

Printer-friendly Version

Interactive Discussion

The transport effects on the short-term component are shown in the probability distributions of both high short-term component values and O₃ exceedances for each wind direction. During the high-O₃ season (May–October) in South Korea, the probabilities of both high short-term component O₃ and O₃ exceedances are higher in the near-westerly wind condition rather than in other wind directions. For the short-term time-scale, the eastward long-range transport of O₃ and precursors from China can cause the nationwide high probabilities of O₃ exceedances in the near-westerly wind condition. However, the high probabilities of O₃ extreme events in downwind regions of the thermoelectric power plants and industrial complexes are related to local transport of O₃ precursors which apparently enhances the O₃ levels.

The distribution of O₃ trends in South Korea is spatially inhomogeneous. Although the relative contributions of the long-term components are much smaller than those of other two components, such spatially inhomogeneous distribution of O₃ trend is mainly contributed by the long-term component O₃ trends rather than the seasonal component O₃ trend related to the long-term change of meteorological conditions. It is because the long-term change of the local precursor emission has a localized effect on the long-term O₃ change. SVD between O₃ and NO₂ shows that the long-term variations of O₃ and NO₂ in South Korea have similar temporal evolutions with different spatial patterns. The results of SVD analysis clearly demonstrate the influences of local precursor emissions on the long-term changes in O₃. However, the precise interpretation of the large spatially inhomogeneous distribution in the long-term component O₃ trend is limited due to lack of VOC measurements data.

The KZ-filter is a useful diagnostic tool to reveal the spatio-temporal features of O₃ and its relationship with meteorological variables. General features revealed by the KZ-filter analysis will provide a better understanding of spatial and temporal variations of surface O₃ as well as possible influences of local emissions, transport, and climate change on O₃ levels in South Korea. Our analyses would also be helpful as a reference for the evaluation of chemistry transport models and furthermore for establishing appropriate O₃ control policy.

Acknowledgements. This study has been funded by the Green City Technology Flagship Program of the Korea Institute of Science and Technology. Daekook Youn was supported by Chungbuk National University. Huikyo Lee performed this study as his private venture and is not in the author's capacity as an employee of the Jet Propulsion Laboratory, California Institute of Technology.

References

- Akimoto, H.: Global air quality and pollution, *Science*, 302, 1716–1719, doi:10.1126/science.1092666, 2003.
- Bell, M. L., Goldberg, R., Hogrefe, C., Kinney, P. L., Knowlton, K., Lynn, B., Rosenthal, J., Rosenzweig, C., and Patz, J. A.: Climate change, ambient ozone, and health in 50 US cities, *Climatic Change*, 82, 61–76, doi:10.1007/s10584-006-9166-7, 2007.
- Bernard, S. M., Samet, J. M., Grambsch, A., Ebi, K. L., and Romieu, I.: The potential impacts of climate variability and change on air pollution-related health effects in the United States, *Environ. Health Persp.*, 109, 199–209, 2001.
- Boo, K.-O., Kwon, W.-T., and Baek, H.-J.: Change of extreme events of temperature and precipitation over Korea using regional projection of future climate change, *Geophys. Res. Lett.*, 33, L01701, doi:10.1029/2005GL023378, 2006.
- Carmichael, G. R., Uno, I., Phadnis, M. J., Zhang, Y., and Sunwoo, Y.: Tropospheric ozone production and transport in the springtime in East Asia, *J. Geophys. Res.*, 103, 10649–10671, doi:10.1029/97JD03740, 1998.
- Chatani, S. and Sudo, K.: Influences of the variation in inflow to East Asia on surface ozone over Japan during 1996–2005, *Atmos. Chem. Phys.*, 11, 8745–8758, doi:10.5194/acp-11-8745-2011, 2011.
- Dawson, J. P., Adams, P. J., and Pandis, S. N.: Sensitivity of ozone to summertime climate in the eastern USA: A modeling case study, *Atmos. Environ.*, 41, 1494–1511, doi:10.1016/j.atmosenv.2006.10.033, 2007.
- Dibb, J. E., Talbot, R. W., Scheuer, E., Seid, G., DeBell, L., Lefer, B., and Ridley, B.: Stratospheric influence on the northern North American free troposphere during TOPSE: be as a stratospheric tracer, *J. Geophys. Res.*, 108, 8363, doi:10.1029/2001JD001347, 2003.

Spatio-temporal analyses of surface ozone and meteorology

J. Seo et al.

Title Page

Abstract

Introduction

Conclusions

References

Tables

Figures

⏪

⏩

◀

▶

Back

Close

Full Screen / Esc

Printer-friendly Version

Interactive Discussion



**Spatio-temporal
analyses of surface
ozone and
meteorology**

J. Seo et al.

Title Page

Abstract

Introduction

Conclusions

References

Tables

Figures

◀

▶

◀

▶

Back

Close

Full Screen / Esc

Printer-friendly Version

Interactive Discussion

Jaffe, D. A., Parrish, D., Goldstein, A., Price, H., and Harris, J.: Increasing background ozone during spring on the west coast of North America, *J. Geophys. Res.*, 30, 1613, doi:10.1029/2003GL017024, 2003.

Jin, L., Lee, S.-H., Shin, H.-J., and Kim, Y. P.: A study on the ozone control strategy using the OZIPR in the Seoul Metropolitan Area, *Asian J. Atmos. Environ.*, 6, 111–117, doi:10.5572/ajae.2012.6.2.111, 2012.

Kim, J. Y., Kim, S.-W., Ghim, Y. S., Song, C. H., and Yoon, S.-C.: Aerosol properties at Gosan in Korea during two pollution episodes caused by contrasting weather conditions, *Asia-Pacific, J. Atmos. Sci.*, 48, 25–33, doi:10.1007/s13143-012-0003-9, 2012.

KMOE (Ministry of Environment, Korea): Annual report of ambient air quality in Korea, 2011, 11-1480523-000198-10, National Institute of Environment Research, Environment Research Complex, Incheon, available at: <http://webbook.me.go.kr/DLi-File/091/012/5515496>. PDF (last access: 15 January 2014), 2012 (in Korean).

KMOE (Ministry of Environment, Korea): Air pollutants emission (1999–2010), 11-1480523-001377-01, National Institute of Environment Research, Environment Research Complex, Incheon, available at: <http://webbook.me.go.kr/DLi-File/NIER/09/018/5553596.pdf> (last access: 15 January 2014), 2013 (in Korean).

Lei, H. and Wang, J. X. L.: Sensitivities of NO_x transformation and the effects on surface ozone and nitrate, *Atmos. Chem. Phys. Discuss.*, 13, 21961–21988, doi:10.5194/acpd-13-21961-2013, 2013.

Levy, H., Mahlman, J., Moxim, W. J., and Liu, S.: Tropospheric ozone: the role of transport, *J. Geophys. Res.*, 90, 3753–3772, doi:10.1029/JD090iD02p03753, 1985.

Levy, J. I., Chemerynski, S. M., and Sarnat, J. A.: Ozone exposure and mortality: an empiric Bayes metaregression analysis, *Epidemiology*, 16, 458–468, doi:10.1097/01.ede.0000165820.08301.b3, 2005.

Lin, C. Y. C., Jacob, D. J., and Fiore, A. M.: Trends in exceedances of the ozone air quality standard in the continental United States, 1980–1998, *Atmos. Environ.*, 35, 3217–3228, doi:10.1016/S1352-2310(01)00152-2, 2001.

Lin, J.-T., Patten, K. O., Hayhoe, K., Liang, X.-Z., and Wuebbles, D. J.: Effects of future climate and biogenic emissions changes on surface ozone over the United States and China, *J. Appl. Meteorol. Clim.*, 47, 1888–1909, doi:10.1175/2007JAMC1681.1, 2008.

Liu, S. C., Trainer, M., Fehsenfeld, F. C., Parrish, D. D., Williams, E. J., Fahey, D. W., Hübler, G., and Murphy, P. C.: Ozone production in the rural troposphere and the im-

**Spatio-temporal
analyses of surface
ozone and
meteorology**

J. Seo et al.

Title Page

Abstract

Introduction

Conclusions

References

Tables

Figures

⏪

⏩

◀

▶

Back

Close

Full Screen / Esc

Printer-friendly Version

Interactive Discussion

plications for regional and global ozone distributions, *J. Geophys. Res.*, 92, 4191–4207, doi:10.1029/JD092iD04p04191, 1987.

Logan, J. A.: Tropospheric ozone: seasonal behavior, trends and anthropogenic influence, *J. Geophys. Res.*, 90, 463–482, doi:10.1029/JD090iD06p10463, 1985.

5 Lu, H. C. and Chang, T. S.: Meteorologically adjusted trends of daily maximum ozone concentrations in Taipei, Taiwan, *Atmos. Environ.*, 39, 6491–6501, doi:10.1016/j.atmosenv.2005.06.007, 2005.

Lu, G. Y. and Wong, D. W.: An adaptive inverse-distance weighting spatial interpolation technique, *Comput. Geosci.*, 34, 1044–1055, doi:10.1016/j.cageo.2007.07.010, 2008.

10 Mickley, L. J., Jacob, D. J., and Field, B. D.: Climate response to the increase in tropospheric ozone since preindustrial times: a comparison between ozone and equivalent CO₂ forcings, *J. Geophys. Res.*, 109, D05106, doi:10.1029/2003JD003653, 2004.

Milanchus, M. L., Rao, S. T., and Zurbenko, I. G.: Evaluating the effectiveness of ozone management efforts in the presence of meteorological variability, *J. Air Waste Manage.*, 48, 201–215, doi:10.1080/10473289.1998.10463673, 1998.

15 Nagashima, T., Ohara, T., Sudo, K., and Akimoto, H.: The relative importance of various source regions on East Asian surface ozone, *Atmos. Chem. Phys.*, 10, 11305–11322, doi:10.5194/acp-10-11305-2010, 2010.

Oh, I. B., Kim, Y. K., Lee, H. W., and Kim, C. H.: An observational and numerical study of the effects of the late sea breeze on ozone distributions in the Busan metropolitan area, Korea, *Atmos. Environ.*, 40, 1284–1298, doi:10.1016/j.atmosenv.2005.10.049, 2006.

20 Oh, I. B., Kim, Y. K., Hwang, M. K., Kim, C. H., Kim, S., and Song, S. K.: Elevated ozone layers over the Seoul Metropolitan Region in Korea: Evidence for long-range ozone transport from eastern China and its contribution to surface concentrations, *J. Appl. Meteorol. Clim.*, 49, 203–220, doi:10.1175/2009JAMC2213.1, 2010.

Olszyna, K. J., Luria, M., and Meagher, J. F.: The correlation of temperature and rural ozone levels in southeastern USA, *Atmos. Environ.*, 31, 3011–3022, doi:10.1016/S1352-2310(97)00097-6, 1997.

25 Ordóñez, C., Mathis, H., Furger, M., Henne, S., Hüglin, C., Staehelin, J., and Prévôt, A. S. H.: Changes of daily surface ozone maxima in Switzerland in all seasons from 1992 to 2002 and discussion of summer 2003, *Atmos. Chem. Phys.*, 5, 1187–1203, doi:10.5194/acp-5-1187-2005, 2005.

Spatio-temporal analyses of surface ozone and meteorology

J. Seo et al.

Title Page

Abstract

Introduction

Conclusions

References

Tables

Figures

⏪

⏩

◀

▶

Back

Close

Full Screen / Esc

Printer-friendly Version

Interactive Discussion

- Racherla, P. N. and Adams, P. J.: Sensitivity of global tropospheric ozone and fine particulate matter concentrations to climate change, *J. Geophys. Res.*, 111, D24103, doi:10.1029/2005JD006939, 2006.
- Rao, S. T. and Zurbenko, I. G.: Detecting and tracking changes in ozone air quality, *J. Air Waste Manage.*, 44, 1089–1092, doi:10.1080/10473289.1994.10467303, 1994.
- Rao, S. T., Zalewsky, E., and Zurbenko, I. G.: Determining temporal and spatial variations in ozone air quality, *J. Air Waste Manage.*, 45, 57–61, doi:10.1080/10473289.1995.10467342, 1995.
- Rao, S. T., Zurbenko, I. G., Neagu, R., Porter, P. S., Ku, J. Y., and Henry, R. F.: Space and time scales in ambient ozone data, *B. Am. Meteorol. Soc.*, 78, 2153–2166, doi:10.1175/1520-0477(1997)078<2153:SATSIA>2.0.CO;2, 1997.
- Rasmussen, D. J., Fiore, A. M., Naik, V., Horowitz, L. W., McGinnis, S. J., and Schultz, M. G.: Surface ozone–temperature relationships in the eastern US: a monthly climatology for evaluating chemistry-climate models, *Atmos. Environ.*, 47, 142–153, doi:10.1016/j.atmosenv.2011.11.021, 2012.
- Shin, H. J., Cho, K. M., Han, J. S., Kim, J. S., and Kim, Y. P.: The effects of precursor emission and background concentration changes on the surface ozone concentration over Korea, *Aerosol Air Qual. Res.*, 12, 93–103, doi:10.4209/aaqr.2011.09.0141, 2012.
- Sillman, S. and Samson, P. J.: Impact of temperature on oxidant photochemistry in urban, polluted rural and remote environments, *J. Geophys. Res.*, 100, 11497–11508, doi:10.1029/94JD02146, 1995.
- Tang, G., Li, X., Wang, Y., Xin, J., and Ren, X.: Surface ozone trend details and interpretations in Beijing, 2001–2006, *Atmos. Chem. Phys.*, 9, 8813–8823, doi:10.5194/acp-9-8813-2009, 2009.
- Tanimoto, H., Sawa, Y., Matsueda, H., Uno, I., Ohara, T., Yamaji, K., Kurokawa, J., and Yone-mura, S.: Significant latitudinal gradient in the surface ozone spring maximum over East Asia, *Geophys. Res. Lett.*, 32, L21805, doi:10.1029/2005GL023514, 2005.
- Tanimoto, H., Ohara, T., and Uno, I.: Asian anthropogenic emissions and decadal trends in springtime tropospheric ozone over Japan: 1998–2007, *Geophys. Res. Lett.*, 36, L23802, doi:10.1029/2009GL041382, 2009.
- Thompson, M. L., Reynolds, J. R., Cox, L. H., Guttorp, P., and Sampson, P. D.: A review of statistical methods for the meteorological adjustment of tropospheric ozone, *Atmos. Environ.*, 35, 617–630, doi:10.1016/S1352-2310(00)00261-2, 2001.

Spatio-temporal analyses of surface ozone and meteorology

J. Seo et al.

Title Page

Abstract

Introduction

Conclusions

References

Tables

Figures

⏪

⏩

◀

▶

Back

Close

Full Screen / Esc

Printer-friendly Version

Interactive Discussion

Tilmes, S. and Zimmermann, J.: Investigation on the spatial scales of the variability in measured near-ground ozone mixing ratios, *Geophys. Res. Lett.*, 25, 3827–3830, doi:10.1029/1998GL900034, 1998.

5 Tsakiri, K. G. and Zurbenko, I. G.: Prediction of ozone concentrations using atmospheric variables, *Air Qual. Atmos. Health*, 4, 111–120, doi:10.1007/s11869-010-0084-5, 2011.

Vingarzan, R.: A review of surface ozone background levels and trends, *Atmos. Environ.*, 38, 3431–3442, doi:10.1016/j.atmosenv.2004.03.030, 2004.

10 Wang, T., Wei, X. L., Ding, A. J., Poon, C. N., Lam, K. S., Li, Y. S., Chan, L. Y., and Anson, M.: Increasing surface ozone concentrations in the background atmosphere of Southern China, 1994–2007, *Atmos. Chem. Phys.*, 9, 6217–6227, doi:10.5194/acp-9-6217-2009, 2009.

Wang, X. and Mauzerall, D. L.: Characterizing distributions of surface ozone and its impact on grain production in China, Japan and South Korea: 1990 and 2020, *Atmos. Environ.*, 38, 4383–4402, doi:10.1016/j.atmosenv.2004.03.067, 2004.

15 Wise, E. K. and Comrie, A. C.: Extending the Kolmogorov-Zurbenko filter: Application to ozone, particulate matter, and meteorological trends, *J. Air Waste Manage.*, 55, 1208–1216, doi:10.1080/10473289.2005.10464718, 2005.

Spatio-temporal analyses of surface ozone and meteorology

J. Seo et al.

Table 1. 12 yr averaged concentrations and temporal linear trends of daily average O₃ (O_{3avg}) at 46 cities over South Korea for the period 1999–2010. The cities are categorized into three groups: 16 coastal cities, 14 inland cities, and 16 cities in the Seoul Metropolitan Area (SMA).

Coastal region	City code	O _{3avg} (ppbv)	Trend (% yr ⁻¹)	Inland region	City code	O _{3avg} (ppbv)	Trend (% yr ⁻¹)	SMA	City code	O _{3avg} (ppbv)	Trend (% yr ⁻¹)
Busan*	BS	23.2	0.65	Andong	AD	22.0	1.35	Ansan	–	20.5	1.81
Changwon	CW	25.1	1.62	Cheonan	CN	18.7	0.72	Anyang	–	16.8	0.67
Gangneung	GN	26.5	2.61	Cheongju	CJ	21.0	1.25	Bucheon	–	18.3	1.71
Gimhae	–	24.4	–0.05	Daegu*	DG	19.8	0.77	Ganghwa	GH	30.9	1.12
Gunsan	GS	22.5	0.66	Daejeon*	DJ	20.7	1.21	Goyang	–	19.1	0.77
Gwangyang	–	28.1	–1.28	Gimcheon	–	24.4	2.36	Gunpo	–	19.6	–0.86
Jeju	JJ1	32.6	2.59	Gumi	GM	22.6	3.70	Guri	–	18.1	–0.83
Jinhae	–	31.3	1.03	Gwangju*	GJ	20.5	3.50	Gwacheon	–	17.6	–1.25
Masan	–	25.2	0.85	Gyeongju	–	22.1	–0.27	Gwangmyeong	–	18.0	0.41
Mokpo	MP	30.3	–0.21	Iksan	–	17.7	2.64	Incheon*	IC	19.0	1.45
Pohang	PH	25.7	0.01	Jecheon	JC	21.0	–0.21	Pyeongtaek	–	19.9	2.75
Seosan	SS	27.5	–1.67	Jeonju	JJ2	18.9	2.55	Seongnam	–	18.8	0.66
Suncheon	–	25.7	0.92	Jinju	JJ3	24.0	2.54	Seoul*	SU	17.1	2.82
Ulsan*	US	21.5	1.61	Wonju	WJ	20.7	–0.24	Siheung	–	21.0	2.29
Yeongam	–	28.6	3.58					Suwon	SW	19.3	1.86
Yeosu	YS	28.1	1.18					Uijeongbu	–	19.9	1.46
Coastal averages		26.6	0.88	Inland averages		21.0	1.56	SMA averages		19.6	1.05
Nationwide averages		22.5	1.15								

* Major metropolitan cities in South Korea (Seoul, Busan, Daegu, Incheon, Gwangju, Daejeon, and Ulsan).

[Title Page](#)
[Abstract](#)
[Introduction](#)
[Conclusions](#)
[References](#)
[Tables](#)
[Figures](#)
[Back](#)
[Close](#)
[Full Screen / Esc](#)
[Printer-friendly Version](#)
[Interactive Discussion](#)

Spatio-temporal
analyses of surface
ozone and
meteorology

J. Seo et al.

Title Page

Abstract

Introduction

Conclusions

References

Tables

Figures

◀

▶

◀

▶

Back

Close

Full Screen / Esc

Printer-friendly Version

Interactive Discussion



Table 2. Coefficients of determination (R^2) between baseline of daily 8 h maximum average O_3 (O_{38h}) and baselines of 6 meteorological variables (T_{max} , SI, TD, PS, WS, and RH) at 25 cities over South Korea for the period 1999–2010. The cities are categorized into three groups: 10 coastal cities, 11 inland cities, and 4 cities in the Seoul Metropolitan Area (SMA). Numbers in bold fonts indicate correlations significant at the 95 % level or higher.

	Cities	City code	T_{max}	Coefficients of determination (R^2)				
				SI	TD	PS	WS	RH
Coastal region	Busan ¹	BS	0.147	0.366	0.139	0.222 ²	0.014	0.135
	Changwon	CW	0.224	n/a	0.179	0.335 ²	0.001 ²	0.138
	Gangneung	GN	0.013	0.480	0.000	0.072 ²	0.014	0.008 ²
	Gunsan	GS	0.032	n/a	0.017	0.047 ²	0.002	0.003 ²
	Jeju	JJ1	0.028 ²	0.080	0.069 ²	0.004	0.009	0.141 ²
	Mokpo	MP	0.012	0.263	0.004	0.038 ²	0.047 ²	0.043 ²
	Pohang	PH	0.034	0.404	0.014	0.102 ²	0.043 ²	0.003
	Seosan	SS	0.059	0.495	0.021	0.135 ²	0.001	0.049 ²
	Ulsan ¹	US	0.071	n/a	0.046	0.107 ²	0.035 ²	0.023
	Yeosu	YS	0.093	n/a	0.061	0.140 ²	0.002 ²	0.024
	Averages		0.071	0.348	0.055	0.120 ²	0.017	0.057
Inland region	Andong	AD	0.269	0.544	0.128	0.379 ²	0.004	0.026 ²
	Cheonan	CN	0.400	n/a	0.263	0.479 ²	0.003 ²	0.056 ²
	Cheongju	CJ	0.387	0.666	0.219	0.443 ²	0.052	0.053 ²
	Daegu ¹	DG	0.381	0.621	0.224	0.493 ²	0.002 ²	0.016
	Daejeon ¹	DJ	0.312	0.721	0.160	0.408 ²	0.089	0.062 ²
	Gumi	GM	0.244	n/a	0.116	0.361 ²	0.009 ²	0.038 ²
	Gwangju ¹	GJ	0.274	0.502	0.159	0.315 ²	0.015	0.005 ²
	Jecheon	JC	0.258	n/a	0.137	0.365 ²	0.012	0.108 ²
	Jeonju	JJ2	0.134	0.434	0.060	0.179 ²	0.008 ²	0.038 ²
	Jinju	JJ3	0.199	0.413	0.129	0.238 ²	0.000	0.012
	Wonju	WJ	0.476	0.767	0.312	0.573 ²	0.069	0.018 ²
Averages		0.303	0.584	0.173	0.385 ²	0.024	0.039 ²	
SMA	Ganghwa	GH	0.204	n/a	0.158	0.274 ²	0.190	0.025
	Incheon ¹	IC	0.310	0.501	0.250	0.411 ²	0.019 ²	0.097
	Seoul ¹	SU	0.419	0.580	0.318	0.531 ²	0.009 ²	0.045
	Suwon	SW	0.525	0.703	0.422	0.640 ²	0.009	0.080
Averages		0.364	0.595	0.287	0.464 ²	0.057	0.062	
Nationwide	Averages		0.220	0.502	0.144	0.292 ²	0.026	0.050 ²

¹: Major metropolitan cities in South Korea.

²: Negative correlation.

n/a: Not available observations of SI.

Spatio-temporal analyses of surface ozone and meteorology

J. Seo et al.

Table 3. 12 yr averaged of daily minimum O_3 (O_{3min}) concentrations and daily average wind speeds (WS) at 46 cities over South Korea for the period 1999–2010. The cities are categorized into three groups: 16 coastal cities, 14 inland cities, and 16 cities in the Seoul Metropolitan Area (SMA).

Coastal region	City code	O_{3min} (ppbv)	WS ($m s^{-1}$)	Inland region	City code	O_{3min} (ppbv)	WS ($m s^{-1}$)	SMA	City code	O_{3min} (ppbv)	WS ($m s^{-1}$)
Busan*	BS	8.2	3.38	Andong	AD	5.6	1.61	Ansan	–	5.7	n/a
Changwon	CW	7.9	2.01	Cheonan	CN	4.9	1.79	Anyang	–	3.9	n/a
Gangneung	GN	11.1	2.86	Cheongju	CJ	6.0	1.70	Bucheon	–	5.9	n/a
Gimhae	–	7.7	n/a	Daegu	DG	5.6	2.31	Ganghwa	GH	12.9	1.84
Gunsan	GS	8.8	3.07	Daejeon*	DJ	5.7	1.96	Goyang	–	6.2	n/a
Gwangyang	–	12.9	n/a	Gimcheon	–	7.9	n/a	Gunpo	–	4.8	n/a
Jeju	JJ1	15.4	3.31	Gumi	GM	7.1	1.53	Guri	–	4.4	n/a
Jinhae	–	13.3	n/a	Gwangju*	GJ	6.0	2.07	Gwacheon	–	4.8	n/a
Masan	–	8.6	n/a	Gyeongju	–	7.9	n/a	Gwangmyeong	–	5.6	n/a
Mokpo	MP	14.1	3.64	Iksan	–	6.4	n/a	Incheon*	IC	5.2	2.69
Pohang	PH	11.5	2.68	Jecheon	JC	6.1	1.51	Pyeongtaek	–	4.9	n/a
Seosan	SS	12.3	2.66	Jeonju	JJ2	6.5	2.02	Seongnam	–	5.8	n/a
Suncheon	–	9.4	1.16	Jinju	JJ3	8.2	1.37	Seoul*	SU	3.8	2.27
Ulsan*	US	7.5	2.12	Wonju	WJ	5.9	1.09	Siheung	–	6.6	n/a
Yeongam	–	13.7	n/a					Suwon	SW	5.2	1.86
Yeosu	YS	11.5	4.30					Uijeongbu	–	4.9	n/a
Coastal averages		10.9	2.84	Inland averages		6.4	1.72	SMA averages		5.6	2.17
Nationwide averages		7.7	2.26								

* Major metropolitan cities in South Korea.
n/a: Not available observations of wind speed.

[Title Page](#)
[Abstract](#)
[Introduction](#)
[Conclusions](#)
[References](#)
[Tables](#)
[Figures](#)
[⏪](#)
[⏩](#)
[◀](#)
[▶](#)
[Back](#)
[Close](#)
[Full Screen / Esc](#)
[Printer-friendly Version](#)
[Interactive Discussion](#)


Spatio-temporal analyses of surface ozone and meteorology

J. Seo et al.

Title Page

Abstract

Introduction

Conclusions

References

Tables

Figures

◀

▶

◀

▶

Back

Close

Full Screen / Esc

Printer-friendly Version

Interactive Discussion

Table 4. Relative contributions (%) of short-term components ($[O_{3ST}]$), seasonal components ($[O_{3SEASON}]$), and long-term components ($[O_{3LT}]$) to total variance of log-transformed daily 8 h maximum average O_3 ($[O_3]$) at 25 cities over South Korea for the period 1999–2010. The cities are categorized into three groups: 10 coastal cities, 11 inland cities, and 4 cities in the Seoul Metropolitan Area (SMA).

Coastal region	City code	Relative contributions (%)			Inland region	City code	Relative contributions (%)			SMA	City code	Relative contributions (%)		
		$[O_{3ST}]$	$[O_{3SEASON}]$	$[O_{3LT}]$			$[O_{3ST}]$	$[O_{3SEASON}]$	$[O_{3LT}]$			$[O_{3ST}]$	$[O_{3SEASON}]$	$[O_{3LT}]$
Busan*	BS	56.1	32.6	2.5	Andong	AD	32.7	53.2	3.6	Ganghwa	GH	56.2	33.1	3.2
Changwon	CW	53.6	36.2	2.0	Cheonan	CN	41.5	46.5	1.8	Incheon*	IC	58.7	32.7	1.5
Gangneung	GN	62.5	29.1	2.0	Cheongju	CJ	48.3	41.7	1.3	Seoul*	SU	51.8	38.2	3.8
Gunsan	GS	52.3	34.2	2.7	Daegu*	DG	50.4	41.3	1.6	Suwon	SW	42.0	49.4	1.8
Jeju	JJ1	53.8	29.2	4.3	Daejeon*	DJ	49.2	40.5	1.5					
Mokpo	MP	46.1	30.9	8.5	Gumi	GM	48.2	42.0	2.7					
Pohang	PH	53.9	34.4	4.1	Gwangju*	GJ	41.5	41.3	4.8					
Seosan	SS	45.1	35.6	5.3	Jecheon	JC	50.8	38.6	4.0					
Ulsan*	US	55.5	32.1	2.5	Jeonju	JJ2	47.4	36.1	4.2					
Yeosu	YS	52.2	34.1	4.3	Jinju	JJ3	55.5	29.2	6.2					
					Wonju	WJ	39.5	50.8	2.3					
Coastal averages		53.1	32.8	3.8	Inland averages		45.9	41.9	3.1	SMA averages		52.2	38.3	2.6
Nationwide averages		49.8	37.7	3.3										

* Major metropolitan cities in South Korea.

Spatio-temporal analyses of surface ozone and meteorology

J. Seo et al.

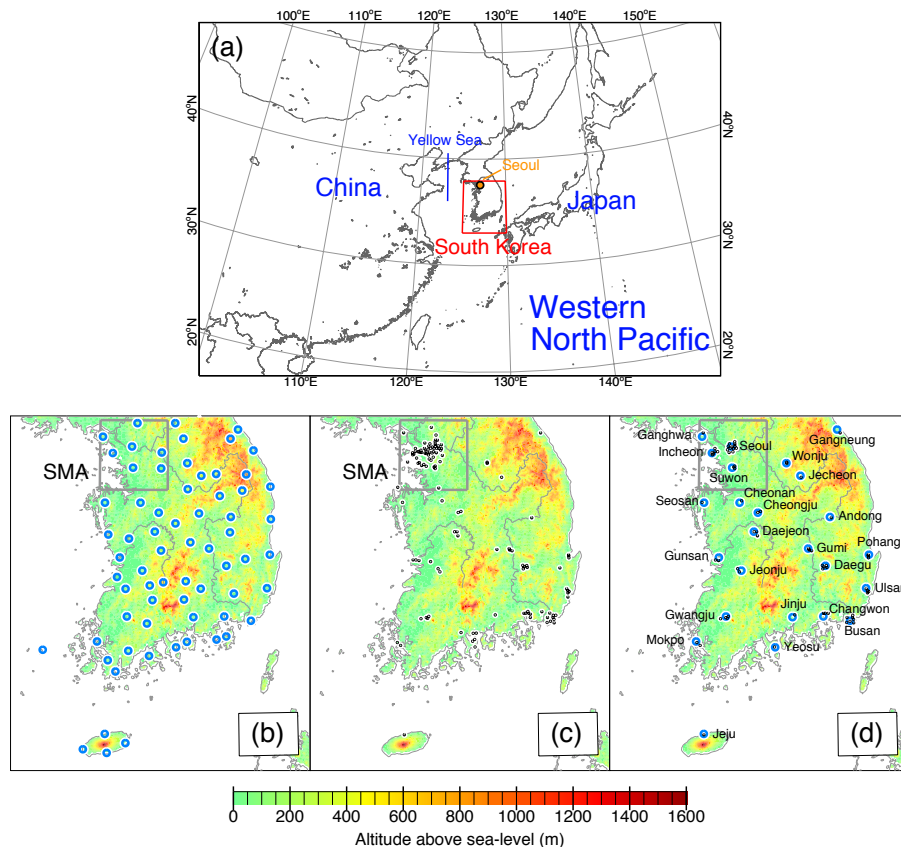


Fig. 1. (a) Geographical locations of South Korea, and (b) 72 weather stations of the Korea Meteorological Administration (KMA) with blue circles, (c) 124 air quality monitoring sites of the National Institute of Environmental Research (NIER) with black dots, and (d) 72 air quality monitoring sites of NIER, which are located within 10 km from 25 weather stations of KMA over the South Korean domain.

Title Page

Abstract

Introduction

Conclusions

References

Tables

Figures

◀

▶

◀

▶

Back

Close

Full Screen / Esc

Printer-friendly Version

Interactive Discussion

Spatio-temporal analyses of surface ozone and meteorology

J. Seo et al.

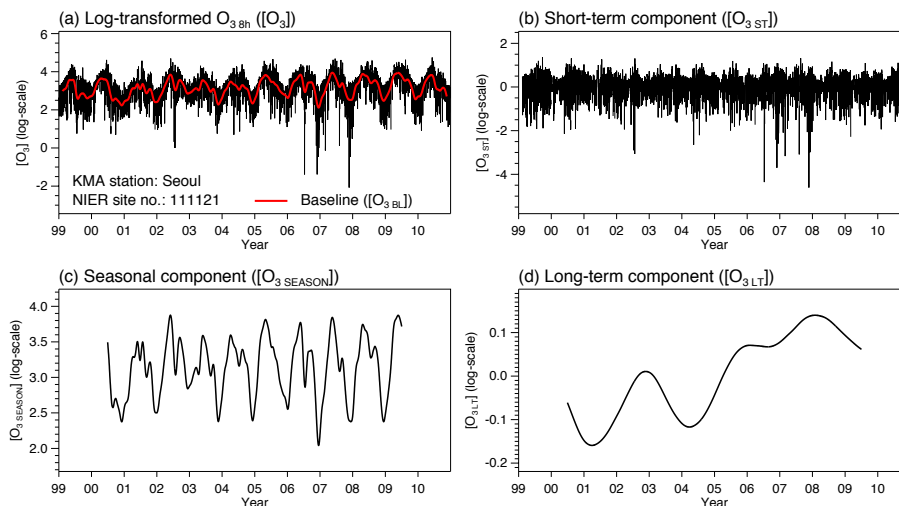


Fig. 2. Time-series of daily 8 h maximum average ozone ($O_{3_{8h}}$) at the City Hall of Seoul and its separated components such as **(a)** log-transformed $O_{3_{8h}}$ time-series ($[O_3]$) and its baseline ($[O_{3_{BL}}]$), **(b)** short-term component ($[O_{3_{ST}}]$), **(c)** seasonal component ($[O_{3_{SEASON}}]$), and **(d)** long-term component ($[O_{3_{LT}}]$) by applying KZ-filter. It is noted that the longer window length causes the larger truncation of the result (Wise and Comrie, 2005) since the KZ-filter is an iterative moving average process. The baseline in red solid line is superimposed in **(a)**.

Title Page

Abstract

Introduction

Conclusions

References

Tables

Figures

◀

▶

◀

▶

Back

Close

Full Screen / Esc

Printer-friendly Version

Interactive Discussion

Spatio-temporal analyses of surface ozone and meteorology

J. Seo et al.

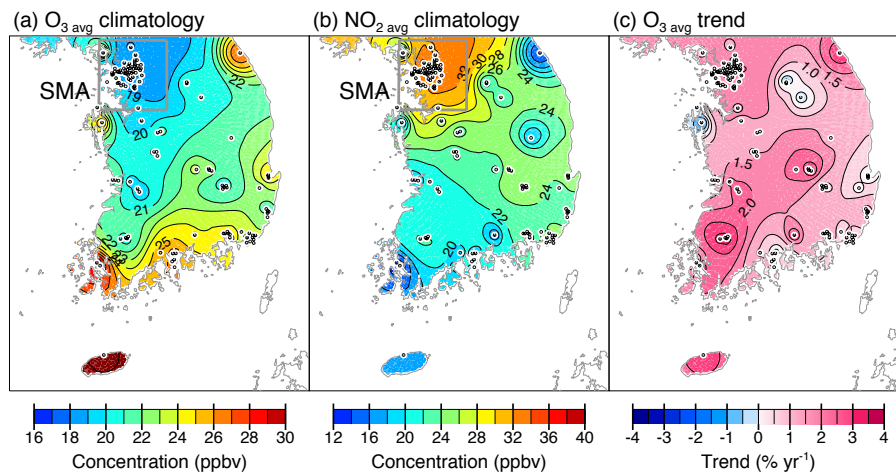


Fig. 3. Spatial distributions of 12 yr averaged concentrations of **(a)** daily average O₃ (O_{3,avg}) and **(b)** daily average nitrogen dioxide (NO_{2,avg}), and **(c)** temporal linear trends of O_{3,avg} for the period 1999–2010 using data from 124 air quality monitoring sites (black dots) of NIER.

[Title Page](#)[Abstract](#)[Introduction](#)[Conclusions](#)[References](#)[Tables](#)[Figures](#)[⏪](#)[⏩](#)[◀](#)[▶](#)[Back](#)[Close](#)[Full Screen / Esc](#)[Printer-friendly Version](#)[Interactive Discussion](#)

Spatio-temporal analyses of surface ozone and meteorology

J. Seo et al.

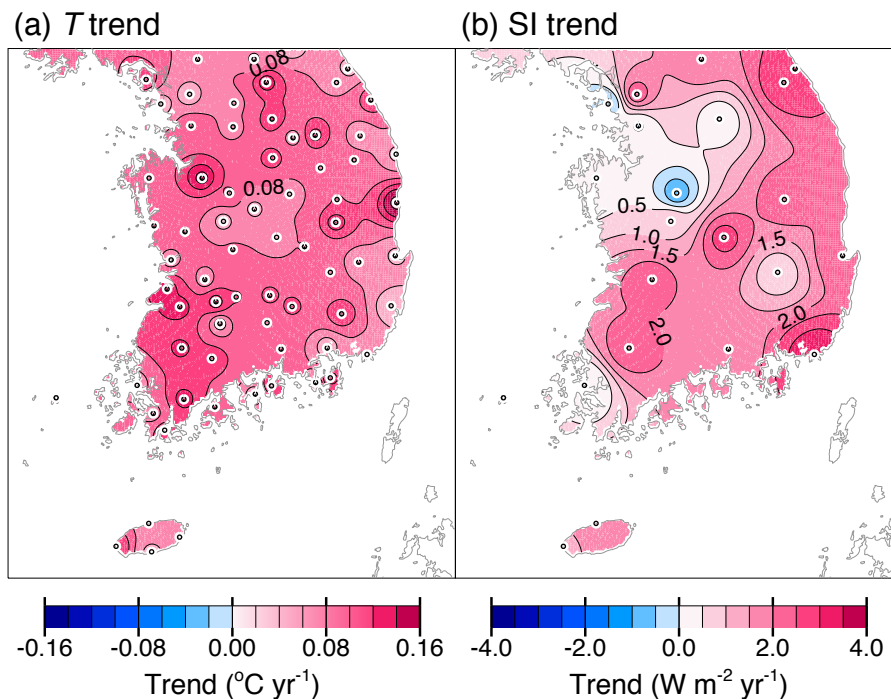


Fig. 4. Spatial distributions of temporal linear trends of (a) daily average temperature (T) and (b) daily average surface insolation (SI) for the period 1999–2010 using data from 72 and 22 weather stations (black dots) of KMA, respectively.

[Title Page](#)[Abstract](#)[Introduction](#)[Conclusions](#)[References](#)[Tables](#)[Figures](#)[⏪](#)[⏩](#)[⏴](#)[⏵](#)[Back](#)[Close](#)[Full Screen / Esc](#)[Printer-friendly Version](#)[Interactive Discussion](#)

Spatio-temporal analyses of surface ozone and meteorology

J. Seo et al.

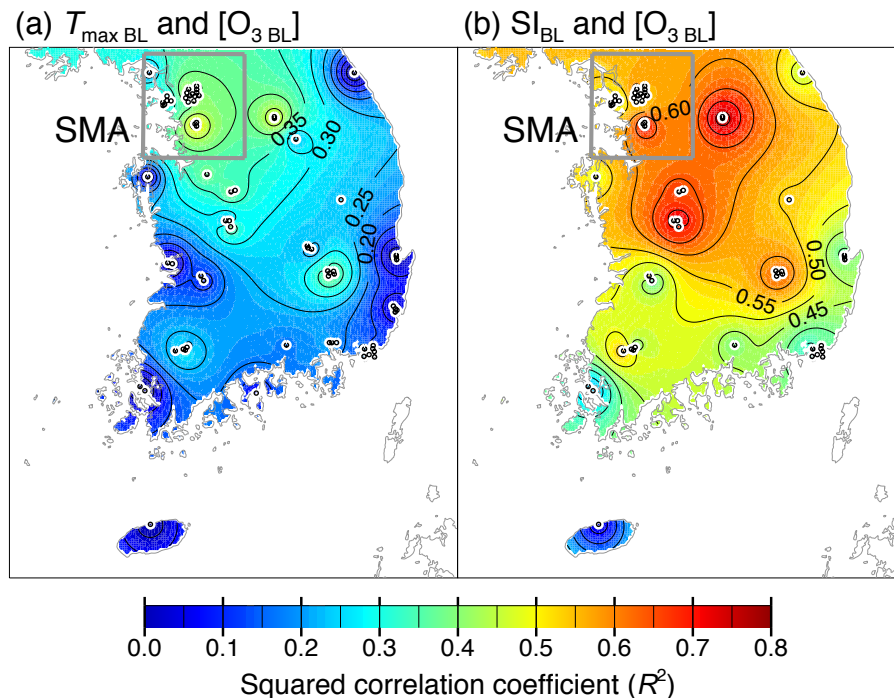


Fig. 5. Spatial distributions of squared correlation coefficients (R^2) between baselines of O_{38h} ($[O_{3BL}]$) and (a) daily maximum temperature (T_{max_BL}) and (b) surface insolation (SI_{BL}). Black dots represent 72 air quality monitoring sites of NIER.

Title Page

Abstract

Introduction

Conclusions

References

Tables

Figures

◀

▶

◀

▶

Back

Close

Full Screen / Esc

Printer-friendly Version

Interactive Discussion

Spatio-temporal analyses of surface ozone and meteorology

J. Seo et al.

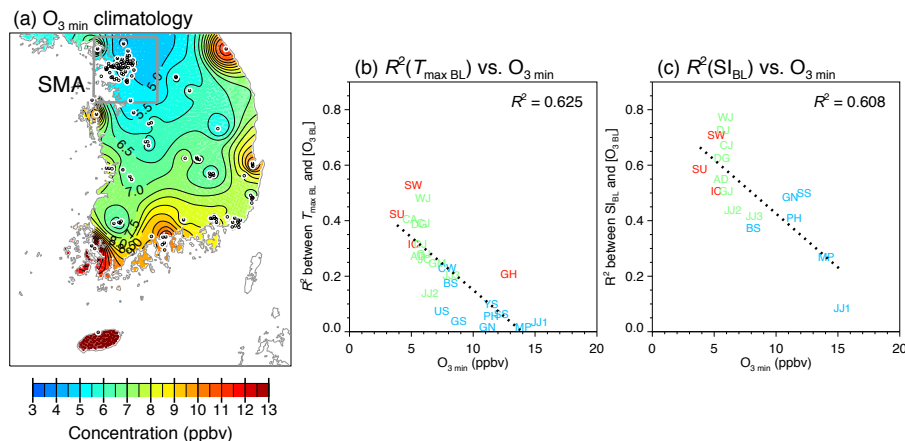


Fig. 6. (a) Spatial distribution of 12 yr averaged concentrations of daily minimum O_3 ($O_{3\min}$) for the period 1999–2010 using data from 124 air quality monitoring sites (black dots) of NIER. (b) Scatter plot of R^2 between $[O_{3BL}]$ and $T_{\max BL}$ vs. $O_{3\min}$ at 25 cities. (c) Scatter plot of R^2 between $[O_{3BL}]$ and SI_{BL} vs. $O_{3\min}$ at 17 cities. City codes in red, green, and blue indicate the Seoul Metropolitan Area (SMA), inland, and coastal cities, respectively.

Title Page

Abstract

Introduction

Conclusions

References

Tables

Figures

◀

▶

◀

▶

Back

Close

Full Screen / Esc

Printer-friendly Version

Interactive Discussion

Spatio-temporal analyses of surface ozone and meteorology

J. Seo et al.

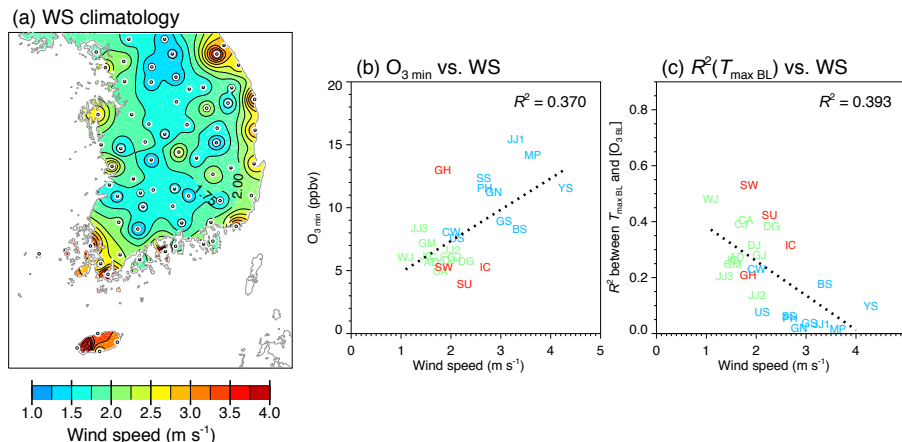


Fig. 7. (a) Spatial distribution of 12 yr averaged daily average wind speeds (WS) for the period 1999–2010 using data from 72 weather stations (black dots) of KMA. **(b)** Scatter plot of $O_{3\min}$ vs. WS at 25 cities. **(c)** Scatter plot of R_2 between $[O_{3BL}]$ and $T_{\max,BL}$ vs. WS at 25 cities. City codes in red, green, and blue indicate the Seoul Metropolitan Area (SMA), inland, and coastal cities, respectively.

Title Page

Abstract

Introduction

Conclusions

References

Tables

Figures

◀

▶

◀

▶

Back

Close

Full Screen / Esc

Printer-friendly Version

Interactive Discussion

Spatio-temporal analyses of surface ozone and meteorology

J. Seo et al.

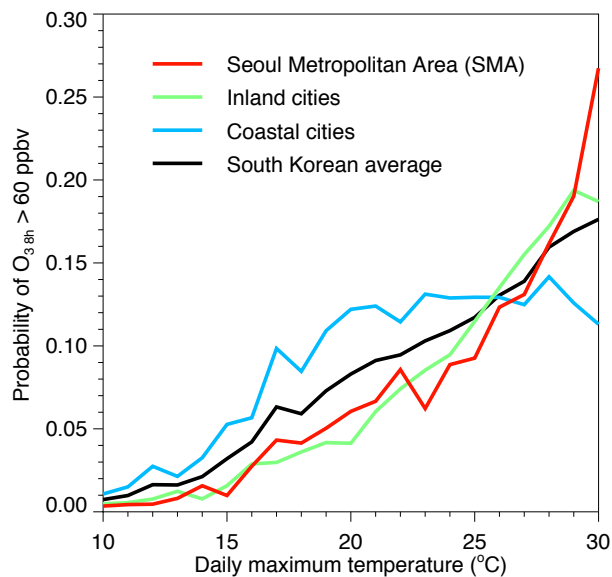


Fig. 8. Probabilities of O_3 exceedances in the given range of daily maximum temperature (T_{max}) that O_{38h} will exceed air quality standard of South Korea (60 ppbv).

Spatio-temporal analyses of surface ozone and meteorology

J. Seo et al.

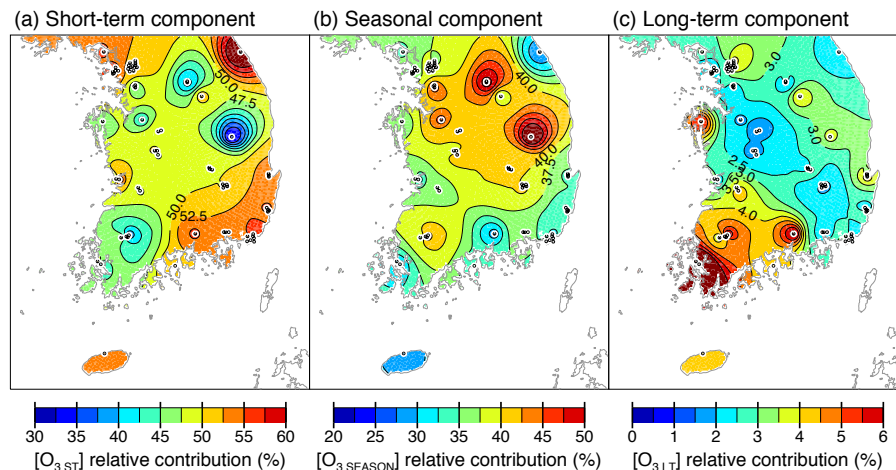


Fig. 9. Spatial distributions of relative contributions of **(a)** short-term component ($[O_{3ST}]$), **(b)** seasonal component ($[O_{3SEASON}]$), and **(c)** long-term component ($[O_{3LT}]$) to the total variance of original time-series ($[O_3]$) using data from 72 air quality monitoring sites (black dots) of NIER. Note that the color scales are all different.

[Title Page](#)[Abstract](#)[Introduction](#)[Conclusions](#)[References](#)[Tables](#)[Figures](#)[◀](#)[▶](#)[◀](#)[▶](#)[Back](#)[Close](#)[Full Screen / Esc](#)[Printer-friendly Version](#)[Interactive Discussion](#)

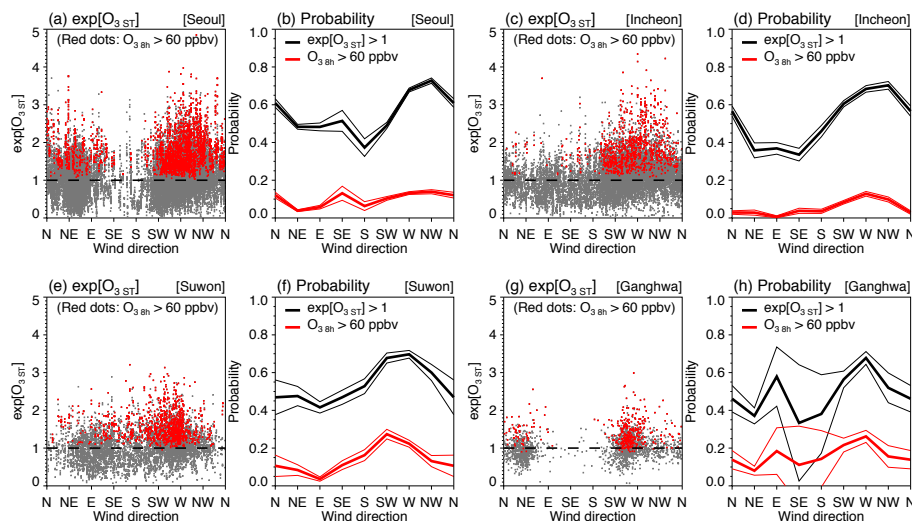


Fig. 10. Relationships between wind directions (WD) and exponentials of short-term components ($\exp[\text{O}_{3\text{ST}}]$) during the high- O_3 season (May–October) at Seoul (a–b), Incheon (c–d), Suwon (e–f), and Ganghwa (g–h) in the Seoul Metropolitan Area (SMA) are represented in scatter plots of $\exp[\text{O}_{3\text{ST}}]$ vs. WD (a, c, e and g) and probabilities of O_3 exceedances in each WD (b, d, f and h). Red dots in scatter plots denote high- O_3 episodes that daily 8 h maximum average O_3 ($\text{O}_{38\text{h}}$) will exceed air quality standard of South Korea (60 ppbv). Dashed lines in scatter plots denote the reference of $\exp[\text{O}_{3\text{ST}}] = 1$. Probabilities of $\exp[\text{O}_{3\text{ST}}] > 1$ and $\text{O}_{38\text{h}} > 60$ ppbv in each WD are represented as black thick lines and red thick lines, respectively. 95 % of confidence intervals for each probability are represented as black and red thin lines. We used O_3 data from 12 sites in Seoul, 6 sites in Incheon, 3 sites in Suwon, and 1 site in Ganghwa.

[Title Page](#)
[Abstract](#)
[Introduction](#)
[Conclusions](#)
[References](#)
[Tables](#)
[Figures](#)
[◀](#)
[▶](#)
[◀](#)
[▶](#)
[Back](#)
[Close](#)
[Full Screen / Esc](#)
[Printer-friendly Version](#)
[Interactive Discussion](#)

Spatio-temporal analyses of surface ozone and meteorology

J. Seo et al.

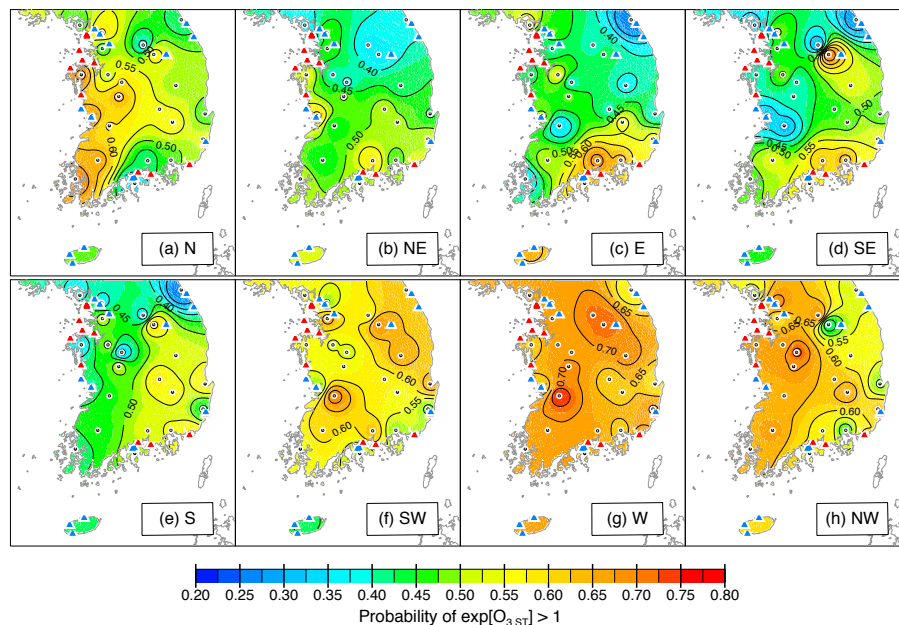


Fig. 11. Spatial distributions of probabilities that exponentials of the short-term components will exceed 1 ($\exp[\text{O}_{3\text{ST}}] > 1$) for each wind direction (WD) of **(a)** northerly (N), **(b)** northeasterly (NE), **(c)** easterly (E), **(d)** southeasterly (SE), **(e)** southerly (S), **(f)** southwesterly (SW), **(g)** westerly (W), and **(h)** northwesterly (NW), respectively. Black dots denote 25 weather stations of KMA and triangles denote 26 major thermoelectric power plants in South Korea (blue triangle < 1000 MW, red triangles ≥ 1000 MW).

Title Page

Abstract

Introduction

Conclusions

References

Tables

Figures

◀

▶

◀

▶

Back

Close

Full Screen / Esc

Printer-friendly Version

Interactive Discussion

Spatio-temporal analyses of surface ozone and meteorology

J. Seo et al.

Title Page

Abstract

Introduction

Conclusions

References

Tables

Figures

◀

▶

◀

▶

Back

Close

Full Screen / Esc

Printer-friendly Version

Interactive Discussion

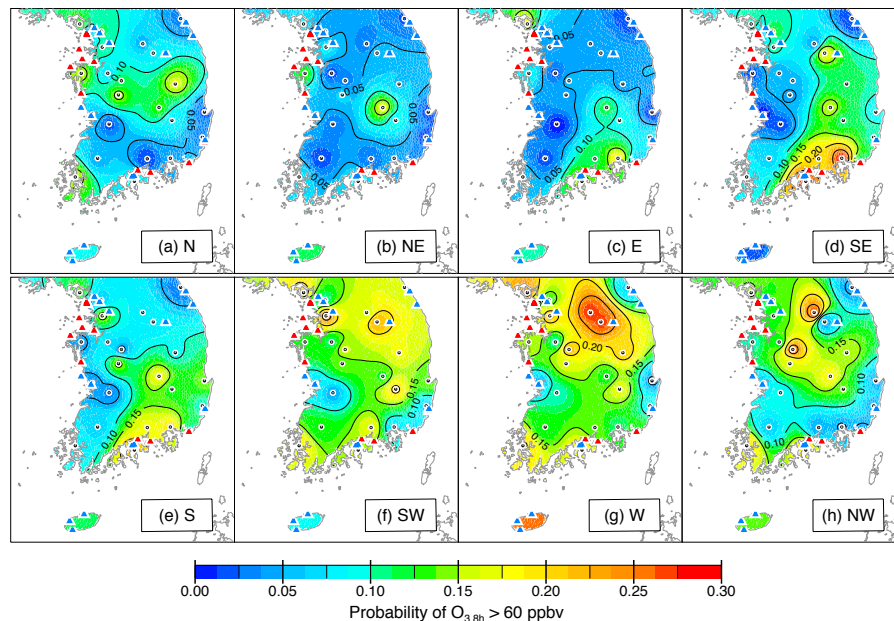


Fig. 12. Spatial distributions of probabilities that daily 8 h maximum average O_3 ($O_{3_{8h}}$) will exceed air quality standard of South Korea (60 ppbv) for each wind direction (WD) of **(a)** northerly (N), **(b)** northeasterly (NE), **(c)** easterly (E), **(d)** southeasterly (SE), **(e)** southerly (S), **(f)** southwesterly (SW), **(g)** westerly (W), and **(h)** northwesterly (NW), respectively. Black dots denote 25 weather stations of KMA and triangles denote 26 major thermoelectric power plants in South Korea (blue triangle < 1000 MW, red triangles \geq 1000 MW).

Spatio-temporal analyses of surface ozone and meteorology

J. Seo et al.

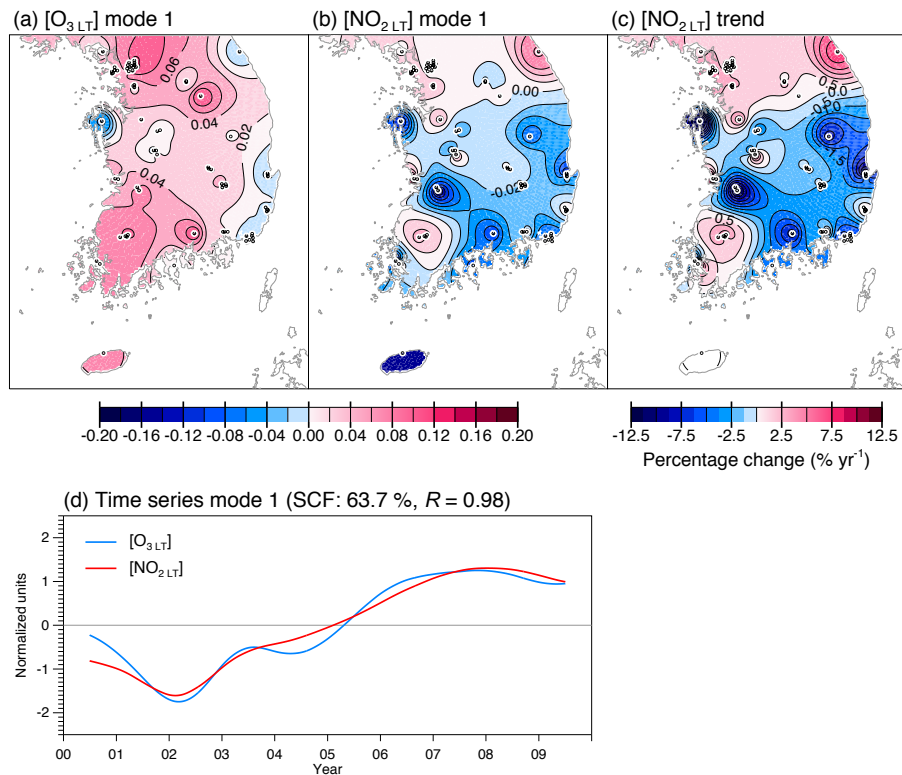


Fig. 14. The first leading mode of SVD between the long-term components of **(a)** daily 8 h maximum average O_3 ($[O_{3LT}]$) and **(b)** daily average NO_2 ($[NO_{2LT}]$) for the period 2000–2009. **(c)** Spatial distribution of temporal linear trends of $[NO_{2LT}]$. **(d)** Time-series of the SVD expansion coefficient associated with $[O_{3LT}]$ mode (blue line) and $[NO_{2LT}]$ mode (red line).